Evaluation and Improvement of Coastal GNSS Reflectometry Sea Level Variations from Existing GNSS Stations in Taiwan

Chi–Ming Lee[1], Chung–Yen Kuo[1,*], Jian Sun[2], Tzu–Pang Tseng[3,4], Kwo–Hwa Chen[5], Wen–Hau Lan[1], C.K. Shum[2,6], Tarig Ali[7], Kuo–En Ching[1], Philip Chu[8], Yuanyuan Jia[2]

[1]Department of Geomatics, National Cheng Kung University, No. 1, University Road, Tainan City 701, Taiwan

[2]Division of Geodetic Science, School of Earth Sciences, Ohio State University, Columbus, OH 43210, USA

[3]Cooperative Research Centre for Spatial Information, Australia, Level 5, 204 Lygon St, Carlton VIC 3053, Australia

[4]Geoscience Australia, Australia, Cnr Jerrabomberra Ave and Hindmarsh Drive, Symonston ACT 2609, Australia

[5]Department of Real Estate and Built Environment, National Taipei University, Taiwan.

[6]Institute of Geodesy & Geophysics, CAS, Wuhan, China.

[7]Geospatial Analysis Center, American University of Sharjah, United Arab Emirates (UAE).

[8]NOAA Great Lakes Environmental Research Laboratory, National Oceanic and Atmospheric Administration, Ann Arbor, Michigan, USA.

[*] Correspondence: kuo70@mail.ncku.edu.tw

+886-6-2757575 ext. 63826

ABSTRACT

Global sea level rise due to an increasingly warmer climate has begun to induce hazards, adversely affecting the lives and properties of people residing in low-lying coastal regions and islands. Therefore, monitoring and understanding variations in coastal sea level covering offshore regions are of great importance. Signal-to-noise ratio (SNR) data of Global Navigation Satellite System (GNSS) have successfully used to robustly derive sea level heights (SLHs). In Taiwan, there is a number of continuously operating GNSS stations, not originally installed for sea level monitoring. They were established in harbors or near coastal regions for monitoring land motion. This study utilizes existing SNR data from three GNSS stations (Kaohsiung, Suao, and TaiCOAST) in Taiwan to compute SLHs with two methods, namely, Lomb–Scargle Periodogram (LSP)-only, and LSP aided with tidal harmonic analysis developed in this study. The results of both methods are compared with co-located or nearby tide gauge records. Owing to the poor quality of SNR data, the worst accuracy of SLHs derived from traditional LSP-only method exceeds 1 meter at the TaiCOAST station. With our procedure, the standard deviations (STDs) of difference between GNSS-derived SLHs and tide gauge records in Kaohsiung and Suao stations decreased to 10 cm and the results show excellent agreement with tide gauge derived relative sea level records, with STD of differences of 7 cm and correlation coefficient of 0.96. In addition, the absolute GNSS-R sea level trend in Kaohsiung during 2006–2011 agrees well with that derived from satellite altimetry. We conclude that the coastal GNSS stations in Taiwan have the potential of monitoring absolute coastal sea level change accurately when our proposed methodology is used.

***Index Terms*—Global navigation satellite systems (GNSS), signal-to-noise ratio (SNR), Lomb-Scargle periodogram (LSP), tidal harmonic analysis**

1. INTRODUCTION

Global sea level rise (SLR) has become increasingly hazardous in some of the low-lying coastal regions over the past decades primarily due to anthropogenic climate warming. The adverse impacts of SLR on the economy and environment of coastal cities and island nations include salinity intrusion, inundation and flooding, coastal erosion, and wetland and habitat destruction for endangered species (Klein and Nicholls, 1999; LaFever et al., 2007; Fuentes et al., 2009). In addition, low-lying coastal regions are the most vulnerable to the threats of SLR. Most of the large and populous cities in the world with their associated economic activities and infrastructures, are situated at or near the coastal and deltaic regions (FitzGerald et al., 2008). Moreover, the population living within 100 km of coasts is predicted to account for half of the global population by 2030 (Small and Nicholls, 2003). Hence, continuous monitoring, understanding and mitigating sea level rise hazards in the world's deltaic and other low-lying coastal areas, are becoming necessary and indispensable.

Traditionally, relative and absolute (geocentric) sea level changes are mainly monitored using tide gauges and satellite altimetry, respective1ly. Although tide gauges can provide high-accuracy measurements up to millimeter level (Míguez et al., 2012), estimated sea level observations in this case contain vertical land motions (VLM), which lead to over- or under-estimates of SLR. For example, tide gauges in Taiwan, especially in the southwestern part, are influenced by significant VLM (Lan et al., 2017). Satellite altimetry can be used for large-scale sea level observations and exhibit accuracy better than ±5 cm in open oceans (Shum et al., 1995). Nevertheless, there is a great challenge when applying this method in coastal regions because waveform contamination of the land and inaccurate geophysical corrections lead to low-accuracy observations (Chelton et al., 2001; Kuo et al., 2017). Furthermore, high temporal resolution and continuous monitoring of the sea surface with satellite altimetry are restricted to the repeat cycle of each satellite. Therefore, an alternative

or supplementary method may be developed to complement the above-mentioned techniques.

Global Navigation Satellite Systems Reflectometry (GNSS-R) is a new satellite technique that has been applied using reflected or opportunistic signals for remote sensing of Earth surfaces. Larson et al. (2013a) introduced GNSS-based tide gauges to measure coastal relative sea level heights (SLHs) by using signal-to-noise ratio (SNR) analysis via Lomb–Scargle Periodogram (LSP) method. Derived relative sea level changes are consistent with those of nearby or collocated tide gauges; the largest root mean square (RMS) is about 10 cm, indicating that GNSS-R has a great potential for monitoring sea level variations offshore and with higher temporal sampling. Löfgren and Haas (2014) showed that SNR analysis can still provide SLHs during rough sea surface conditions (wind speed of up to 17.5 m/s). Hence, a GNSS-based tide gauge could still operate even under challenging conditions. Most importantly, since this technique is GNSS-based, the site can also be used to compute VLM via geodetic positioning, and can thus derive absolute sea level changes that cannot be achieved by traditional tide gauges alone.

The most populated cities on the island of Taiwan are situated close to coasts. Accurate monitoring of sea level changes around Taiwan is therefore important; in this regard, dozens of tide gauges have been established by the Taiwan government (Lan et al., 2017). Three continuous GNSS stations of Taiwan were built to be co-located with tide gauges in harbors or near the coastlines and were not originally intended to be used for GNSS-reflectometry, so they may be not optimal for sea level monitoring compared to other sites chosen in previous studies. The present research aims to assess if these three GNSS stations (Kaohsiung, Suao, and TaiCOAST) could serve as GNSS-based tide gauges. Therefore, we introduce tidal harmonic analysis to assist LSP in deriving accurate SLHs with reasonable precision close to those achieved in previous studies. Finally, GNSS-derived results via LSP-only technique which were used in previous published studies, and via our method are compared with those

from co-located or nearby traditional tide gauge records. Furthermore, GNSS-derived sea level trend combined with VLM for the Kaohsiung GNSS station is compared with the absolute sea level trend obtained from multi-mission satellite altimetry.

2. RESEARCH AREAS AND DATA

In this study, we selected three GNSS stations that are located in Kaohsiung Harbor, Suao Harbor, and Taoyuan (TaiCOAST). Kaohsiung Harbor is the largest commercial port in Taiwan and the 13th largest harbor worldwide. This harbor is adjacent to Kaohsiung City, one of the economic centers in Taiwan. The site consists of a Trimble 5700 GNSS receiver with an unshielded TRM41249.00 antenna mounted on the top of a building at pier 10. Suao Harbor is situated in the Yilan County, one of the auxiliary ports of Keelung commercial port, and plays a critical role in the development of Lan–Yang Plain, where most people in Yilan reside. The GNSS station consists of a Trimble NETR9 receiver and a TRM57971.00 antenna. TaiCOAST is a sea-front tower facing Taiwan Strait and was established by National Central University, Taoyuan, Taiwan. TaiCOAST is a 16 m-high (about five floors) building with few shelters, and the field of vision here is wide and broad. The receiver is a NovAtel GPS Card with a GPS-702-GG antenna. The approximate heights of the antennae above mean sea level of Kaohsiung, Suao and TaiCOAST are 5.34 m, 4.40 m and 20.26 m, respectively. The co-located or nearby traditional tide gauges are selected to verify GNSS-based tide gauges. Figure 1 illustrates the geographical locations of these stations. Tables 1 and 2 list GNSS stations and tide gauges information. Two types of data used in this research; SNR data recorded by GNSS receivers and tide gauge measurements. SNR data are collected in GPS L1 and L2 carrier frequencies, only SNR-L1 data are used in this study because the signal strength of SNR-L2 data is relatively weaker. The relative sea level measurements of the four tide gauges are used to validate GNSS-derive sea level changes. Tidal harmonic analysis is applied to detect outliers or datum offsets in the tide gauge records prior to its use for the validation of GNSS-R retrieved sea level data.

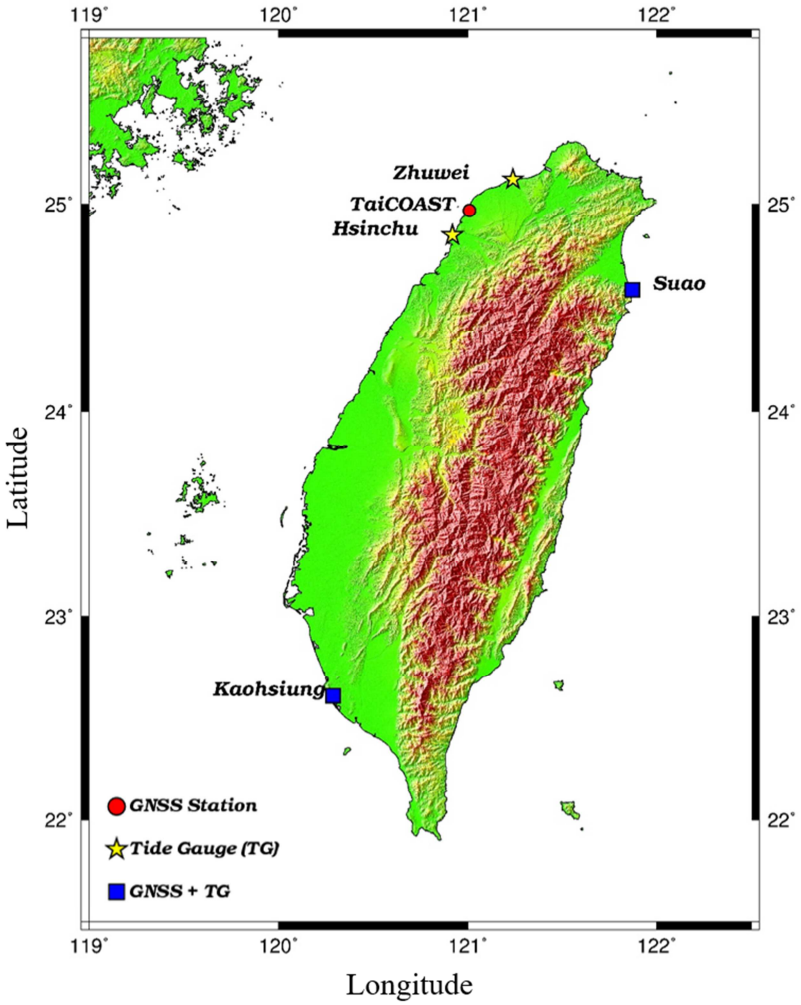

Figure 1. GNSS stations and tide gauges in Taiwan. The red circle represents GNSS stations, the yellow star denotes traditional tide gauges, and the blue square indicates GNSS stations co-located with traditional tide gauges.

Table 1. Information of three GNSS stations

Station	Lon. ($^{\circ}E$)	Lat. ($^{\circ}N$)	Temporal Coverage	Sampling rate (Hz)	Provider
Kaohsiung	120.29	22.61	2006/03/01 –2011/07/31	1/30	Ministry of Interior
Suao	121.87	24.59	2015/11/01 –2015/12/31	1/30	Central Weather Bureau
TaiCOAST	121.01	24.97	2015/07/24 –2015/08/07	1	National Central University

Table 2. Information of four nearby or collocated tide gauges

Station	Lon. ($^{\circ}E$)	Lat. ($^{\circ}N$)	Temporal Coverage	Tidal Range (m)	Provider
Kaohsiung	120.29	22.61	2006/01/01 –2011/12/31	< 1.0	Ministry of Interior
Suao	121.87	24.59	2015/01/01 –2015/12/31	1.0	Central Weather Bureau
Zhuwei	121.24	25.12	2015/06/01 –2015/08/31	2.0	Central Weather Bureau
Hsinchu	120.92	24.85	2015/06/01 –2015/08/31	2.5	Central Weather Bureau

3. METHODOLOGY

3.1. GNSS SNR Theory

SNR recorded by GNSS receivers can be utilized for analyzing multipath effects. Each GNSS frequency, such as L1, L2, or L5, records its own SNR value, which is calculated by carrier tracking loop of the GNSS receiver (Bilich and Larson, 2007). The direct signal component is eliminated from the original SNR data to obtain the signal related to multipath reflections. This process can be achieved either by fitting and removing a low-order polynomial (Larson et al., 2013a) or by designing a high-pass filter for the data (Benton and Mitchell, 2011). Similar to the study of Larson et al. (2013a), we fit and remove a second-order polynomial from the SNR data. The remaining part, namely, detrended SNR (δSNR), contains the contribution of the multipath effects and can be shown for a planar surface (Larson et al., 2013a):

$$\delta SNR = A\cos(\psi + \varphi) = A\cos(\frac{4\pi h}{\lambda}\sin(\varepsilon) + \varphi) \tag{1}$$

where A is the amplitude, ψ represents the phase angle, φ denotes the phase offset, h is the distance between the reflecting surface and the GNSS antenna phase center (also called reflected height), λ is the GNSS carrier wavelength, and ε is the satellite elevation angle. The frequency of δSNR with respect to the *sine* of satellite elevation angle can be shown as Eq. (2):

$$f_{\delta SNR\to\sin(\varepsilon)} = \frac{d\delta SNR}{d\sin(\varepsilon)} = \frac{f_{\psi\to\sin(\varepsilon)}}{2\pi} = \frac{2\dot{h}}{\lambda}\frac{\tan(\varepsilon)}{\dot{\varepsilon}} + \frac{2h}{\lambda} \tag{2}$$

Assuming a time-invariant planar surface, that is, the reflected height is constant during a time interval, then $\dot{h}$ can be neglected and Eq. (2) can be simplified as follows:

$$f_{\delta SNR \to x} = \frac{2h}{\lambda}$$

$$h = \frac{f_{\delta SNR \to x}\lambda}{2} \tag{3}$$

Eq. (3) shows that the reflected height is proportional to the oscillation frequency of δSNR data with respect to the *sine* of the satellite elevation angle. The dominant frequency is determined through a spectral analysis method. If the assumption of a constant reflected height in a specific time span is not acceptable in the area where the sea level changes dramatically, then the frequency of δSNR is time dependent. Larson et al. (2013b) mentioned the problem in their study in an experimental area (Kachemak Bay, Alaska) with tidal range larger than 7 m. In this situation, the change rate of the reflected height and satellite elevation angle in Eq. (2) should be considered. Larson et al. (2013b) dealt with this issue by proposing an iterative method. They first calculated the preliminary reflected height solution by Eq. (3), and the correction term to the reflected height is then determined based on $\dot{h}$ and $\tan(\varepsilon)/\dot{\varepsilon}$. Finally, the procedure is repeated to obtain accurate solutions.

3.2. Constraints of SLH derived from SNR Data

Before retrieving SLHs, we need to confirm that the SNR data are truly obtained from surrounding sea surfaces. Therefore, the satellite angle constraints including azimuth and elevation angles are implemented in this research. First, the azimuth angle, which is directly related to the environmental conditions of the GNSS station, is directly determined from a Google Earth image to identify the range facing the sea surfaces. Second, we adopt and calculate the first Fresnel zone of each site to determine the constraints of satellite elevation angle and similar to Löfgren and Haas (2014). Table 3 lists the angle constraints of each station in this study.

Table 3. Angle constraints to SNR data of each GNSS station

Station	Azimuth angle	Elevation angle
Kaohsiung	$40^\circ - 200^\circ$	$4^\circ - 20^\circ$
Suao	$130^\circ - 260^\circ$	$4^\circ - 20^\circ$
TaiCOAST	$240^\circ - 30^\circ$	$5^\circ - 20^\circ$

3.3. Lomb-Scargle Periodogram aided with Tidal Harmonic Analysis

3.3.1. Lomb-Scargle Periodogram

We need to compute the dominant frequency of δSNR data by spectral analysis. Applying a Fast Fourier Transformation (FFT) or other traditional spectral analysis methods is a great challenge because the δSNR data are not evenly sampled with respect to $\sin\varepsilon$. Therefore, we utilize the Lomb-Scargle Periodogram (LSP), also called least-squares spectral analysis, to analyze periodicities of unevenly sampled dataset (Larson et al., 2013a). The details of LSP are given in (Press et al., 1992):

The dominant frequency corresponds to the largest spectral power and can be transferred to reflected height using Eq. (3). Periodograms from PRN 08 and PRN 11 at Kaohsiung station with reflected heights of around 5 m in DOY 121 and DOY 123, 2009 are shown in Figure 2 (a). However, one significant peak does not always exist in the periodogram because of data quality or contamination by other reflected signals near the GNSS station. In Figure 2 (b), two dominant peaks are found, but the correct reflected height during the period is difficult to distinguish using a simple highest peak criterion. Therefore, we introduce tidal harmonic analysis to aid LSP to determine the correct peak and reflected height.

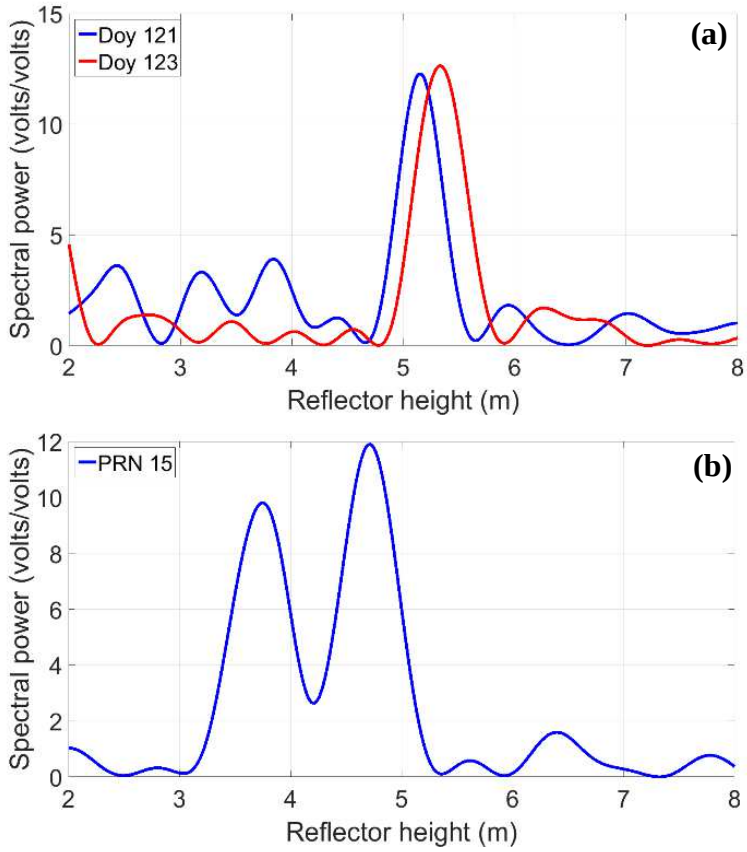

Figure 2. (a) Typical LSP results (only one significant peak) of DOY 121 and DOY 123, 2009 from PRN 08 and PRN 11 with reflected heights 5.15 and 5.33 m, respectively. (b) Non-typical LSP result from an arc of satellite PRN 15 which shows several peaks in the periodogram.

3.3.2. Tidal Harmonic Analysis

In this study, we apply tidal harmonic analysis for two purposes: (i) preprocess tide gauge records to remove datum offsets and blunders, therefore, 37 major tidal constituents are used including 1 annual constituent (SA), 1 semi-annual term (SSA), 3 long-term constituents (MM, MSF, and MF), 10 diurnal tides (2Q1, Q1, RHO, O1, M1, P1, S1, K1, J1, and OO1), 12 semi-diurnal tides (2N2, MU2, N2, NU2, M2, LAM2, L2, T2, S2, R2, K2, and 2SM2), 3 third-diurnal tides (2MK3, M3, and MK3), 4 sixth-diurnal tides (MN4, M4, MS4, and S4), 2 quarter-diurnal tides (M6 and S6), and 1 third-diurnal tide (M8) (Chang et al., 2012). (ii)

LSP-only method used in previous studies cannot generate reasonable results because of the uncertainty or lack of exact knowledge for the peaks estimated in the periodogram (see previous Section *3.3.1*.).

Therefore, we introduced tidal harmonic analysis to constrain the reflected heights (tidal harmonic analysis is ONLY applied to GNSS-R sea surface heights, and the *independent* tide gauges records are then only used for validation). First, we used LSP to retrieve GNSS-R sea level heights, the so-called LSP-only solutions. Then, these LSP-only solutions are used as the input data in tidal harmonic analysis and then reconstruct the sea surface heights. In this way, we can use the reconstructed result to provide a constraint for the reflected height, windowing the periodogram search interval to be optimal or more reasonable. This process has increased the probability for finding the correct peaks. Moreover, the proposed method is iterated until the reconstructed result by tidal harmonic analysis only changes slightly, and the algorithm has demonstrated improvement to the retrieved GNSS reflected heights. In this analysis, we only selected the dominant diurnal (K1 and O1) and semi-diurnal (M2 and S2) tidal constituents because they are significant around Taiwan. The other reason is since the LSP-only solutions are temporally coarse, and could not completely resolve or identify all the known tidal constituents in the tidal harmonic analysis. In addition, if the tidal range of the area is known from tide models, this *a priori* information can be considered as a constraint to accurately determine the peaks in the periodogram. Further, this technique aims to improve the LSP search of peaks to improve GNSS-R sea surface heights, and it is not a tidal modeling study. We find that the use of these 4 dominant tidal constituents is sufficient and more efficient here.

4. RESULTS AND DISCUSSION

4.1. Sea level height (SLH)

GNSS-derived sea level variations by LSP-only and LSP aided with tidal harmonic analysis are compared with those of co-located or nearby tide gauges. The mean value of each time series is removed because they refer to different datums. For TaiCOAST, we just used LSP-only to retrieve SLHs because the intertidal zone appeared during the low tides (Figure 3) which can lead to the wrong detection of reflected heights. Hence, the tidal harmonic analysis cannot be used for the determination of reflected heights because of the wrong fitting result when the input data do not contain the low-tide information. Figure 4 (a)–(c) shows the sea levels of Kaohsiung, Suao and TaiCOAST stations. Tables 4 and 5 present the result for LSP-only and LSP aided with tidal harmonic analysis, respectively. In Kaohsiung and Suao, the standard deviation (STD) of the differences between GNSS-derived and tide gauge sea levels decrease by 7 and 10 cm respectively; the correlation coefficients between the two time series increase from 0.80 to 0.97 when applying LSP aided with tidal harmonic analysis. In addition, the number of sea level estimates increase from 421 to 642 and from 921 to 1171 at Kaohsiung and Suao respectively. It indicates the proposed method increases the probability of finding the correct peaks in the periodgram, and thus significantly improves the retrieved GNSS-R heights for the example GNSS sites. For TaiCOAST, the STD is over 1 m and the correlation coefficient is only 0.13, making it the worst site in Taiwan. The main reason is that when the sea surface ebbs, the distance from the GNSS station to the seawater can reach 300 m or more; that is, outside of the first Fresnel zones. In addition, during the observation period, the sea surface experienced spring tide, when the tidal range is the largest. Therefore, the sea surface height would change dramatically and that affects the performance of SLH retrieval. Another factor causing the discrepancy of the sea level changes between synthetic tide gauge and GNSS-based ide gauge is that the nearby tide

gauges, namely Zhuwei and Hsinchu, which can still observe low tide, are located at the zones with different tidal ranges.

Table 4. Comparison of GNSS-derived sea level changes by LSP-only and tide gauge records.

	Kaohsiung	Suao	TaiCOAST
Number of solutions	421	921	139
STD	15.0 cm	20.0 cm	112.2 cm
Mean diff.	2.1 cm	-0.1 cm	-25.3 cm
Max. diff.	98.3 cm	100.1 cm	316.2 cm
Correlation coefficient	0.80	0.86	0.13

Table 5. Comparison of GNSS-derived sea level changes by LSP aided with the tidal harmonic analysis and tide gauge records with different sea surface assumption.

	Kaohsiung		Suao	
Sea surface assumption	Static	Dynamic	Static	Dynamic
Number of solutions	642	641	1171	1168
STD	7.5 cm	7.1 cm	11.1 cm	9.9 cm
Mean diff.	0.2 cm	0.3 cm	0.1 cm	< 0.0 cm
Max. diff	23.9 cm	24.3 cm	48.3 cm	49.2 cm
Correlation coefficient	0.95	0.96	0.96	0.97

Figure 3. *In-situ* photos of (a) flood tide, and (b) ebb tide at TaiCOAST

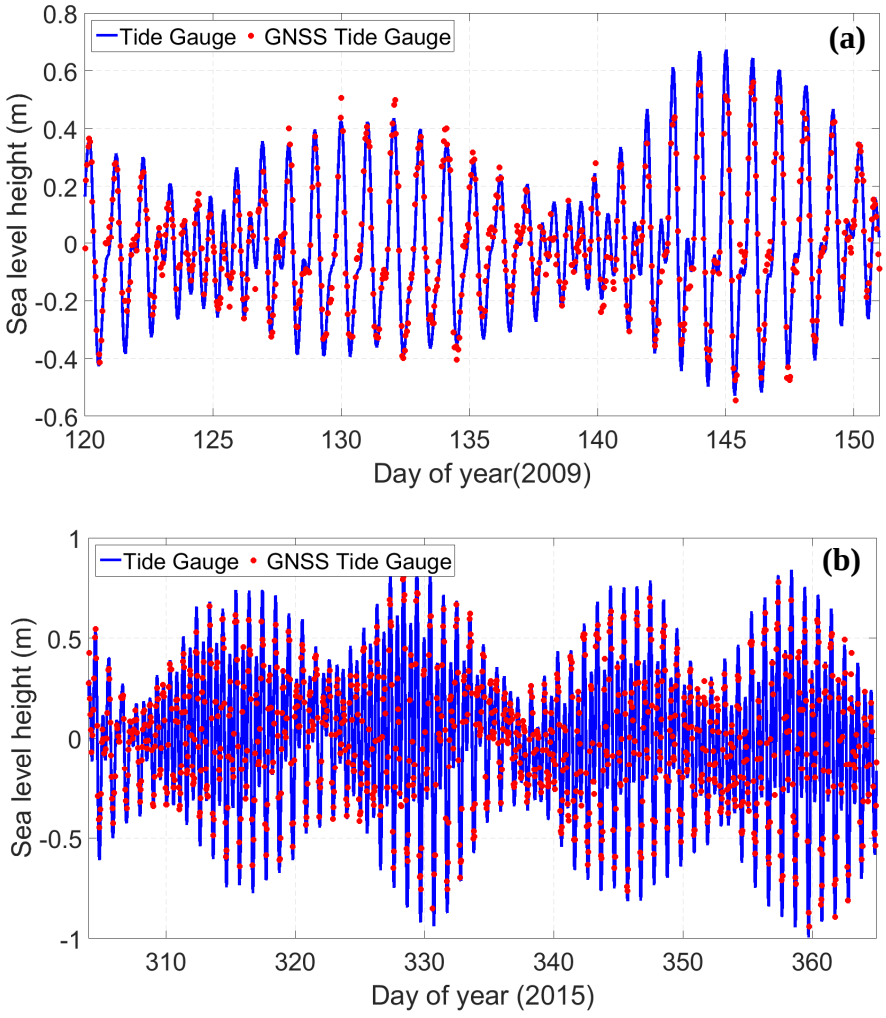

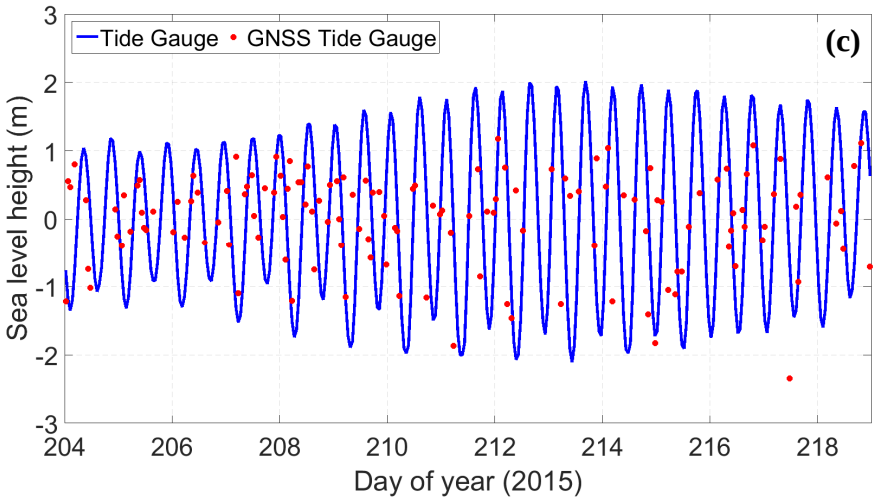

Figure 4. Sea level changes from tide gauge (blue line) and GNSS-based tide gauge with the assumption of dynamic sea surface by LSP with the tidal harmonic analysis (red dot). (a) One-month result from Kaohsiung station, (b) two-month result from Suao harbor, and (c) two-week result from TaiCOAST.

Figure 5 (a)–(b) shows the scatter plots of Kaohsiung and Suao stations, and some solutions are missing in the highest and lowest tides. This finding could be due to lack of available satellites, LSP cannot precisely detect the peak frequency because of the low temporal resolution (1/30 Hz) of the SNR data or the solutions are eliminated via blunder detection. Hence, the estimated slope of linear regression cannot be equal to 1, i.e., the same as the line: y=x. However, the coefficients of determination R^2 are still higher than 0.90. Hence, GNSS-based tide gauge exhibits a high potential for monitoring coastal sea level variations.

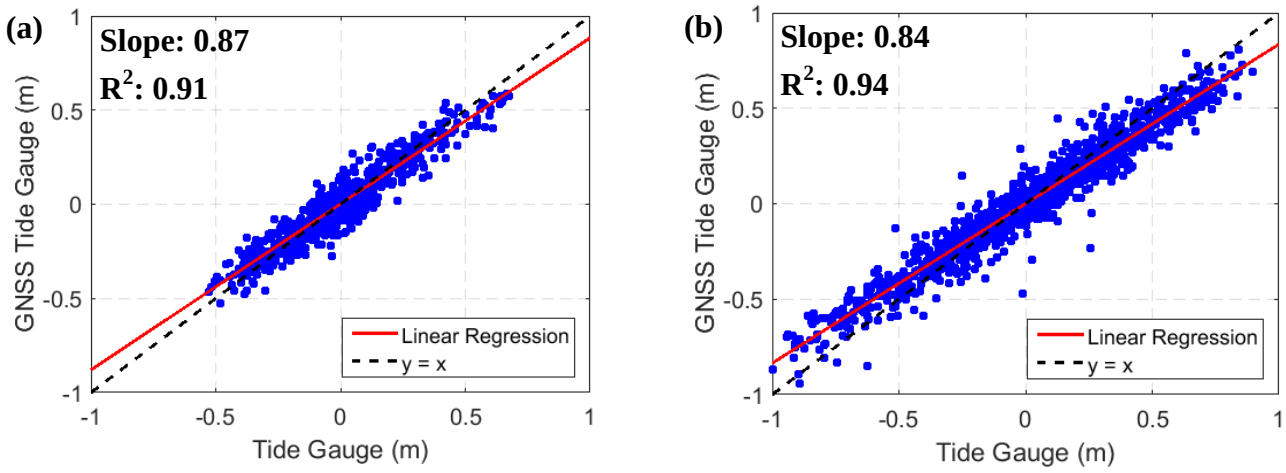

Figure 5. Scatter plot of two sea-level time series from tide gauge and GNSS-based tide gauge by LSP aided with tidal harmonic analysis. (a) Kaohsiung station, (b) Suao station. The red line represents the result of linear regression, and the black line denotes the line: x=y.

4.2. Absolute sea level trend

We also calculate SLHs by using 5-year (2006/03/01-2011/07/31) GNSS SNR data from Kaohsiung station to test the possibility of longer sea level monitoring using the GNSS-based tide gauge. From this analysis, SLHs are valid with an RMS at about 9.0 cm and the correlation coefficient of 0.94. Then, we aimed to compute the absolute sea level trend by removing the VLM from both the relative sea level trends derived from traditional and GNSS-based tide gauges. In addition, along-track absolute sea level changes from TOPEX/POSIEDON, Jason-1 and Jason-2 within 2° from AVISO around the GNSS station are computed for comparison. Figure 6 shows the monthly sea level changes derived from three instruments. The RMS of differences between the tide gauge and GNSS-based tide gauge, the tide gauge and altimeter, and the GNSS-based tide gauge and altimeter are 2.4, 5.8, and 5.9 cm, respectively. Table 6 lists the estimated amplitude and phase of annual and semi-annual variations. The results from tide gauge and GNSS-R retrieval are consistent. The altimeter shows a larger discrepancy compared with the other parameters because the altimeter does not exactly measure the same location as the tide gauge.

The VLM rate used in this study is determined using the GPS vertical components (updated from Ching et al., 2011). The trend of VLM during 2006–2012 is -1.4 ± 0.1 mm/yr. The absolute sea level trend is derived by removing VLM from the tide gauge or GNSS-derived relative sea level trend. Table 7 shows the computed trends of relative and absolute sea levels. The sea level trends derived from GNSS-based tide gauge and satellite altimetry are both negative while it is positive in traditional tide gauge measurements. However, the uncertainty of each estimated trend is larger than its estimate resulting from data covering short time span (5 years), which is not long enough to compute the sea level trend accurately, therefore, the trends are not significantly different. It should be noticed that the trend is calculated using only 5-year data, so the estimated trend contains the uncertainties resulting from low-frequency oceanic signals. The minimum time span of 30 years to obtain reliable sea level trends is suggested by Douglas (1995).

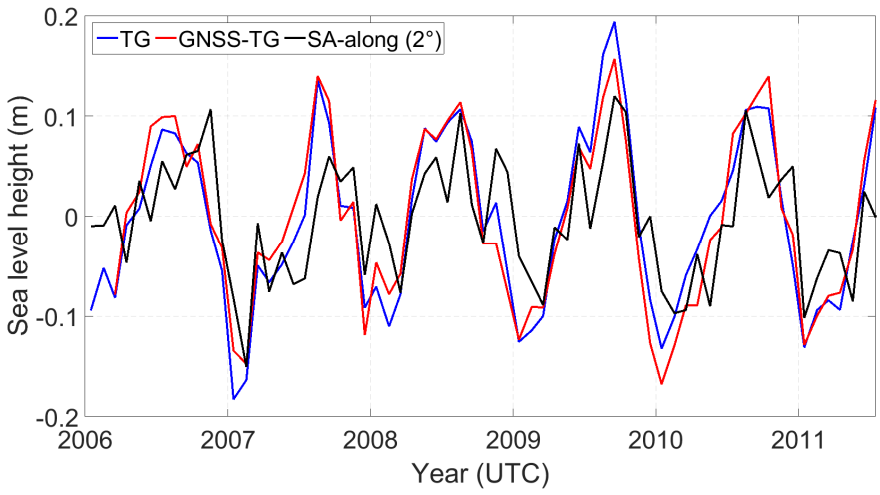

Figure 6. Monthly sea level changes covering 5 years from tide gauge (blue line), GNSS-based tide gauge (red line), and satellite altimetry-along track (2°) (black line).

Table 6. Sea level amplitude and phase of the annual and semi-annual signals

Signal	Annual signal		Semi-annual signal	
parameters	Amplitude (cm)	Phase (◦)	Amplitude (cm)	Phase (◦)
Tide gauge	10.8	208.3	1.9	152.6
GNSS-based tide gauge	11.0	204.6	1.2	147.6
Satellite altimetry	5.9	238.5	1.1	202.3

Table 7. Relative and absolute sea level trends derived from tide gauge, GNSS-based tide gauge, and satellite altimetry

Data source	Relative sea level trend	Absolute sea level trend
Traditional tide gauge	1.9 ± 2.5 mm/y	0.5 ± 2.5 mm/y
GNSS-based tide gauge	-2.5 ± 3.1 mm/y	-3.9 ± 3.1 mm/y
Satellite altimetry – AVISO	N/A	-2.3 ± 3.1 mm/y

4.3. Installation suggestion for GNSS-R Sea Level Station

The set-up of the GNSS station and surrounding environments are important factors that can affect the performance of a GNSS-R sea level station for monitoring sea level variations. The freighters or ships in commercial harbors (Kaohsiung and Suao) or ports will influence the reflected signals from the sea surface. In addition, the GNSS station should be as close to the coastline as possible to avoid multipath from other reflecting surfaces. Otherwise, the reflected signals can be easily affected by other multipath, for example, intertidal zones in TaiCOAST. Furthermore, the sampling rate can affect the maximum reflected height derived by LSP. Therefore, the higher sampling rate is required when the GNSS receiver is built relatively high above the measured sea level (TaiCOAST is the case in this study). These comparisons can provide some principles for future installation of GNSS-based tide gauges.

5. CONCLUSIONS

This study assessed the feasibility of monitoring absolute coastal sea level changes by using the existing data of three GNSS stations in Taiwan. SLHs derived from the SNR data of Kaohsiung and Suao using LSP-only and LSP aided with tidal harmonic analysis are demonstrated, whereas TaiCOAST SNR data are processed using LSP-only. LSP-aided with tidal harmonic analysis increases the probability to find the correct peaks and therefore decreases the STD of difference to 10 cm, indicating significant improvement in GNSS-R sea level height retrievals. Hence, Kaohsiung and Suao GNSS sites have great potential for the feasibility monitoring absolute sea level variations offshore. GNSS-derived sea level changes show high correlation coefficients of 0.94–0.97, in comparison with the co-located traditional tide gauge records for these two GNSS stations. The STDs of the differences between sea level changes derived from GNSS SNR and tide gauge data range from 7.1 to 11.1 cm. Moreover, the absolute sea level trend during 2006–2011 is determined using satellite altimetry measurements or Kaohsiung GNSS SNR data and tide gauge combined with VLM derived from GNSS. The absolute differences in sea level trends are insignificant. However, the uncertainty of each estimated trend is as large as its estimate because the data only cover 5 years, which is not long enough to obtain accurate sea level trends.

The performance of SNR data in TaiCOAST is worse than those at Kaohsiung and Suao. The STD of differences between GNSS-derived and tide gauge sea level is 112.2 cm, and the correlation coefficient is only 0.13. The poor performance is due to multipath from the intertidal zone, not the sea surface. Eventually, statistical comparison of data from previous studies and those from Taiwan’s stations is conducted by LSP aided with tidal harmonic analysis. The result indicates that the existing GNSS stations in Kaohsiung and Suao have great potential for monitoring sea level changes at, around and offshore from the GNSS sites. However, this proposed method may be adversely impacted when the tidal range is

sufficiently large such that the peaks may be skewed or even split when using the LSP.

ACKNOWLEDGMENTS

This research is supported by grants from the Ministry of Science and Technology of Taiwan (MOST 104-2221-E-006-048-MY3 and MOST 106-2119-M-006-018), NASA's GNSS Remote Sensing Program (NNX15AU99G), and NOAA's Cooperative Institute for Great Lakes Research/University of Michigan (3004491689). This is NOAA GLERL Contribution Number 1900. Figure 1 was prepared using the Generic Mapping Tool (GMT) graphics package (Wessel and Smith, 1991).

REFERENCES

Benton, C. J., & Mitchell, C. N. (2011). Isolating the multipath component in GNSS signal-to-noise data and locating reflecting objects. *Radio Science, 46*(6), 1-11, https://dx.doi.org/10.1029/2011RS004767.

Bilich, A., & Larson, K. M. (2007). Mapping the GPS multipath environment using the signal-to-noise ratio (SNR). *Radio Science*, *42*(6), 1-16, https://dx.doi.org/10.1029/2007RS003652.

Chang, E. T., Chao, B. F., Chiang, C. C., & Hwang, C. (2012). Vertical crustal motion of active plate convergence in Taiwan derived from tide gauge, altimetry, and GPS data. *Tectonophysics*, *578*, 98-106, https://dx.doi.org/10.1016/j.tecto.2011.10.002.

Chelton, D. B., Ries, J. C., Haines, B. J., Fu, L. L., & Callahan, P. S. (2001). Satellite altimetry. *International geophysics*, *69*, 1-ii, https://dx.doi.org/10.1016/S0074-6142(01)80146-7.

Ching, K. E., Hsieh, M. L., Johnson, K. M., Chen, K. H., Rau, R. J., & Yang, M. (2011). Modern vertical deformation rates and mountain building in Taiwan from precise leveling and continuous GPS observations, 2000–2008. *Journal of Geophysical Research*, *116*, B08406, https://dx.doi.org/10.1029/2011JB008242.

Douglas, B. C. (1995). Global sea level change: Determination and interpretation. *Reviews of Geophysics*, *33(S2)*, 1425-1432, https://dx.doi.org/10.1029/95RG00355.

Fitzgerald, D. M., Fenster, M. S., Argow, B. A., & Buynevich, I. V. (2008). Coastal Impacts Due to Sea-Level Rise. *Annual Review of Earth and Planetary Sciences*, *36(1)*, 601-647, https://dx.doi.org/10.1146/annurev.earth.35.031306.140139.

Fuentes, M. M. P. B., Limpus, C. J., Hamann, M., & Dawson, J. (2009). Potential impacts of projected sea□level rise on sea turtle rookeries. *Aquatic Conservation: Marine and Freshwater Ecosystems*, *20*(2), 132-139, https://dx.doi.org/10.1002/aqc.1088.

Klein, R. J. T., & Nicholls, R. J. (1999). Assessment of coastal vulnerability to climate change. *Ambio*, *28*(2), 182-187, Retrieved from https://www.jstor.org/stable/4314873.

Kuo, C.Y., Yang, T.Y., Kao, H.C., Wang, C.K., Lan, W.H., & Tseng, H.Z. (2017). Improvement of Envisat altimetric measurements in Taiwan coastal oceans by a developed waveform retracking system. *Journal of Environmental Informatics*, Published online (in press), https://dx.doi.org/10.3808/jei.201500324.

LaFever, D. H., Lopez, R. R., Feagin, R. A., & Silvy, N. J. (2007). Predicting the impacts of future sea-level rise on an endangered lagomorph. *Environmental Management*, *40*(3), 430-437, https://dx.doi.org/10.1007/s00267-006-0204-z.

Lan, W. H., Kuo, C. Y., Kao, H. C., Lin, L. C., Shum, C. K., Tseng, K. H., & Chang, J. C. (2017). Impact of Geophysical and Datum Corrections on Absolute Sea-Level Trends from Tide Gauges around Taiwan, 1993–2015. *Water*, *9*(7), 480, https://dx.doi.org/10.3390/w9070480.

Larson, K. M., Löfgren, J. S., & Haas, R. (2013a). Coastal sea level measurements using a single geodetic GPS receiver. *Advances in Space Research*, *51*(8), 1301-1310, https://dx.doi.org/10.1016/j.asr.2012.04.017.

Larson, K. M., Ray, R. D., Nievinski, F. G., & Freymueller, J. T. (2013b). The accidental tide gauge: a GPS reflection case study from Kachemak Bay, Alaska. *IEEE Geoscience and Remote Sensing Letters*, *10*(5), 1200-1204, https://dx.doi.org/10.1109/LGRS.2012.2236075.

Löfgren, J. S., & Haas, R. (2014). Sea level measurements using multi-frequency GPS and GLONASS observations. *EURASIP Journal on Advances in Signal Processing*, *2014*(1), 50, https://dx.doi.org/10.1186/1687-6180-2014-50.

Míguez, B. M., Testut, L., & Wöppelmann, G. (2012). Performance of modern tide gauges: towards mm-level accuracy. *Scientia Marina*, *76*(S1), 221-228,

https://dx.doi.org/10.3989/scimar.03618.18A.

Press, W. H., Teukolsky, S. A., Vetterling, W. T., Flannery, B. P., & Metcalf M. (1992). *Numerical Recipes in C: The Art of Scientific Computing, Second Edition,* Cambridge University press.

Shum, C. K., Ries, J. C., & Tapley, B. D. (1995). The accuracy and applications of satellite altimetry. *Geophysical Journal International*, *121*(2), 321-336, https://dx.doi.org/10.1111/j.1365-246X.1995.tb05714.x.

Small, C., & Nicholls, R. J. (2003). A global analysis of human settlement in coastal zones. *Journal of Coastal Research*, *19*(3), 584-599, Retrieved from https://www.jstor.org/stable/4299200.

Wessel, P., & Smith, W. H. (1991). Free software helps map and display data. *Eos, Transactions American Geophysical Union*, *72*(41), 441-446, https://dx.doi.org/10.1029/90EO00319.